INTERNATIONAL JOURNAL OF INNOVATIVE RESEARCH & DEVELOPMENT

ISSN 2278 – 0211 (Online)

Anti-Sway Control on a Harbor Crane System Using a Command Smoothing Iterative Method

Roberto Paolo Luigi Caporali
Researcher, Department of R &D, Mathematics for Applied Physics di Roberto Caporali, Italy

Abstract:
The requests for relatively large-sized mobile harbor cranes are increasing. Typically, harbor cranes are self-traveling but do not require any additional civil works to improve the bearing strength of foundation soil. This work describes a novel method able to reduce the sway of a suspended load during the slewing motion of a Harbor Crane. The proposed method is based on an iterative calculation of the sway angle, and the corresponding applied velocity profiles as input to the crane motors. The 'command smoothing' method is used to reduce the sway: additional damping is introduced into the system to control the sway. The multiple-input and multiple-output (MIMO) mechanical system is modeled by a set of non-linear differential equations in which the mathematical model is divided into two subsystems: the first for actuated outputs and the second for underactuated outputs. After defining the stability of the proposed solution and the kinematics of the hydraulic actuators on the boom, a detailed mathematical model is developed, taking into account the non-linear components of the forces, such as centrifugal and Coriolis forces, on the system. Simulation results show that the proposed anti-sway method can dampen the suspended load's oscillations during the harbor crane's slewing movement.

Keywords: *Harbor crane, Anti-sway, Command smoothing, Under-actuated system*

1. Introduction

Cranes can be subdivided into two most important groups: gantry cranes and boom cranes. Boom cranes are industrial structures used in building construction, factories, harbors, and shipyards. Besides, they are used mainly to transport heavy loads in shipyards, factories, and high building construction. These cranes are usually controlled manually because the operators use a joystick and an accelerator pedal to control the movements and direction of the cranes.

Many studies have focused on developing efficient controllers for gantry cranes. In this case, an anti-sway method is easier to develop due to the decoupling among the equations of the movement. In fact, industrial cranes (gantry or overhead cranes) exhibit a one-degree-of-freedom sway in the solution equations. On the contrary, only a limited number of studies have been conducted to design control approaches to reduce the payload sway of boom cranes. This is due to the complexity of the calculations for the motion control.

The recent work of Ramli et al. [1] allows an exhaustive literature review of the strategies relative to crane control and the relative published works. Concerning the studies relating to Anti-sway for Overhead and gantry cranes, we can mention, among many others, the recent works [2] and [3]. Many researchers proposed solutions by developing several control schemes for a crane system. The developed control schemes can be categorized into the open-loop and closed-loop techniques. Numerous researchers have widely utilized open-loop control schemes to control the payload's sway. Open-loop schemes are easy to implement because there is no requirement for additional sensors to measure the sway angles, which certainly saves in terms of cost.

Nevertheless, they are sensitive to external disturbances. External disturbances that always affect a crane's performance are the wind or the sea waves for a crane used on ships. The three main open-loop techniques are input shaping, filtering, and command smoothing. The recent works of the author [4] and [5] are examples of an open-loop technique for sway attenuation on boom (tower) cranes.

With the recent trend toward containerization, it is increasingly essential for local small and medium-sized harbors to use mobile harbor cranes capable of handling containers and other general cargoes in different ways. Therefore, demands for large-sized mobile harbor cranes, which are self-traveling and versatile but do not require any additional civil works to increase the foundation soil, are increasing. In this work, we developed a method for harbor crane systems with an anti-sway function using a Command smoothing method in an open loop.

In the last years, a few papers have been done to investigate the sway of the payload for a Harbor (boom) crane. Some works concern the study of harbor cranes in the open sea. We can see, for example, the recent works of D. Kim et al. [6] and Y.G. Sun et al. [7]. This kind of work is highly complex because it is necessary to consider disturbances such as waves and wind. In this case, the Mobile Harbor has 6 degrees of freedom motion because of external disturbances such as waves and wind.

We will limit ourselves to studying Harbor cranes on the fixed surface, on land, not on the sea. Therefore, we are simplifying the problem in this case. In particular, we want to highlight four recent and essential works regarding Harbor cranes on the land. The works of E. Arnold et al. [8], J. Neupert et al. [9], T. Toyohara et al. [10], D. Kim et al. [11], and J. Huang et al. [12] define the problem of studying an optimal control approach or an alternative feedback control system (closed-loop control).

As part of the study relative to the anti-sway control of harbor crane systems, we investigated the stability of the solution we defined. In fact, only when the solution defined is obtained as a stable solution can we discuss its performance and operating characteristics. In a recent paper [13], the author demonstrated the stability of his solution, obtained under particular conditions.

In general, our solution for controlling a harbor crane is in the context of underactuated systems. In practice, many control problems involve the underactuated behavior of mechanical systems. In underactuated systems, the number of equipped actuators is less than that of the controlled variables. That is, actuators do not directly control some degrees of freedom. Within the scope of the Harbor crane system we studied, the underactuated variables turn out to be the 'sway' variables, that is, the sway angles in the tangential and normal direction to the slewing rotation of the boom.

In the analysis of the stability of the anti-sway system related to Harbor cranes, we will refer to the following fundamental works. The works we cite are those of L.A. Tuan et al. [14], L.A. Tuan et al. [15], and M.W. Spong [16]. In addition, E. Lefeber et al. [17] investigated tracking control for underactuated ships in which three state variables, a surge, sway, and yaw, were controlled by only two inputs: surge force and yaw torque.

This paper is organized as follows.

In Section 2, the dynamical model of the Harbor crane is described. The harbor crane is modeled, defining a multi-body system including base, mast (fixed vertical column), boom, and payload.

Section 3 gives a mathematical description of a generic Underactuated system and the Stability Analysis for the same system.

In Section 4, a mathematical description of a Harbor crane is defined. From Lagrange equations, the five dynamical equations relative to the two sway angles (underactuated system) and the other lagrangian variables (actuated system) are obtained, including the dissipation function. Also, Stability Analysis for a harbor crane and Hydraulic cylinder cinematics are given.

In Section 5, the Equations solution is obtained, describing the used iterative method.

An implementation of the theory defined in Section 6 is given, and the most relevant results of the model simulation are presented, with particular emphasis on the fact that total damping is obtained by changing many times the velocity set, also during the previous ramps.

In Section 7, concluding remarks and possible developments are defined in the end.

2. Dynamical Model of a Harbour Crane

A Harbor (boom) crane is a multi-body system including base, mast (fixed vertical column), jib, trolley, and payload. The boom crane system considered in this work is shown in Figure 1, and it is schematized in Figure 2, where x and z represent the base coordinates.

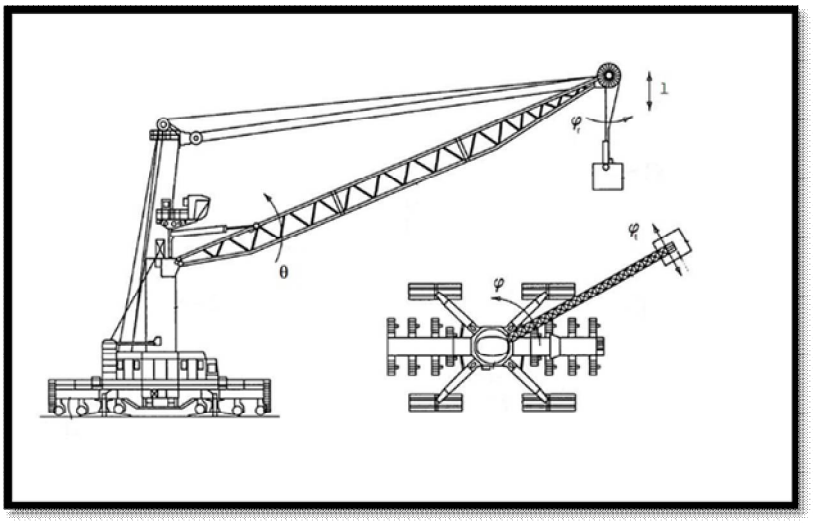

Figure 1: General View of a Harbour Crane. Side and Top View

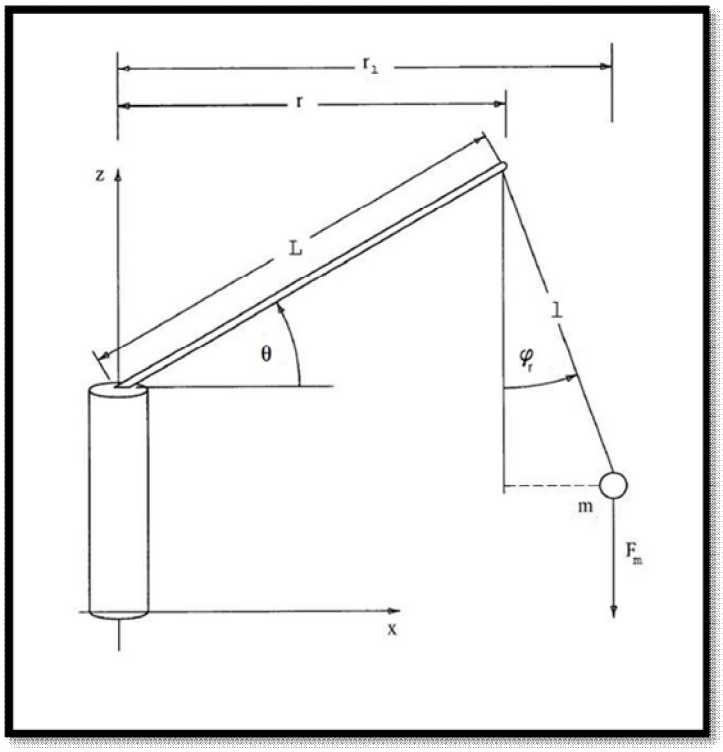

Figure 2: Geometric Description of the Harbour Crane System

The crane system consists of a fixed vertical column, a rigid boom link, a hoisting line, and a payload $\varphi\ \theta$, l representing the slew angle, luff angle, and the length of the hoisting line, respectively. The slew angle is the rotary angle of the hub of the boom crane or slewing pedestal controlled by the operator's slew command, whereas the luff angle is the elevation or luffing angle of the boom link. Sway angles are excited as the system operates, namely the tangential φ_t and radial sway φ_r. In this study, the payload is regarded as a point mass, and the system exhibits the behavior of a pendulum. In the described system with at least one first and one-second strand of cables, both strands of cables extend from the tip of the boom to a suspension element such as a hook. The length of the cable can be adjusted by a corresponding drive to move the load in the vertical direction.

Concerning Figure 2, the dynamics of the generalized Harbor crane are represented as a multi-body system with five independent degrees of freedom, described by five Lagrangian coordinates q_i :

$q_1 = r$ The radial position of the boom extremity on the axis x;

$q_2 = \varphi$ Slewing angle (rotation around the axis z);

$q_3 = l$ Hoisting length of the cable (along the axis z);

$q_4 = \varphi_r$ Sway angle in the radial direction;

$q_5 = \varphi_t$ Sway angle tangential to the trajectory of the slewing direction;

3. Mathematical Description of an under Actuated System and Stability Analysis

We refer to the paper of L.A. Tuan et al. [14] and the paper of the author [13]. In general, the physical behavior of a MIMO mechanical system is governed by a set of differential equations of motion. For example, consider an underactuated system with n degrees of freedom driven by m actuators ($m < n$). The mathematical model, which is composed of n ordinary differential equations, is simplified in matrix form as follows:

$$M(q)\ddot{q} + C(q,\dot{q})\dot{q} + G(q) = Q \quad (1)$$

where $q = [q_1, q_2, ...q_n]^T \in R^n$ is the vector of the generalized coordinates and $Q \in R^n$ denotes the vector of the control inputs. $M(q) = M(q)^T = [m_{i,j}]_{n\,x\,n} \in R^{n\,x\,n}$ is the symmetric mass matrix, $C(q,\dot{q}) = [c_{i,j}]_{m\,x\,n} \in R^{m\,x\,n}$ is the Coriolis and centrifugal matrix, $G(q) = [g_1, g_2, ...g_n]^T \in R^n$ is the gravity vector. Given that the system has more control signals than actuators, Q it has only m non-zero components as $U = [u_1, u_2, ...u_m]^T \in R^m$ being a vector of non-zero input forces. As an underactuated system, its n output signals are driven by m actuators. Its mathematical model is divided into two auxiliary dynamics: actuated and unactuated systems. Correspondingly, we define the generalized coordinates $q_a = [q_1, q_2, ...q_m]^T \in R^m$ for actuated states and $q_u = [q_{m+1}, q_{m+2}, ...q_n]^T \in R^{n-m}$ for unactuated states. The matrix differential equation (1) can be divided into two equations as follows:

$$M_{11}(q)\ddot{q}_a + M_{12}(q)\ddot{q}_u + C_{11}(q,\dot{q})\dot{q}_a + C_{12}(q,\dot{q})\dot{q}_u + G_1(q) = U \quad (2)$$

$$M_{21}(q)\ddot{q}_a + M_{22}(q)\ddot{q}_u + C_{21}(q,\dot{q})\dot{q}_a + C_{22}(q,\dot{q})\dot{q}_u + G_2(q) = 0 \quad (3)$$

Matrices $M(q)$ $C(q,\dot{q})$ and $G(q)$ have the following form:

$$M(q) = \begin{bmatrix} M_{11}(q) & M_{12}(q) \\ M_{21}(q) & M_{22}(q) \end{bmatrix}; \quad C(q,\dot{q}) = \begin{bmatrix} C_{11}(q,\dot{q}) & C_{12}(q,\dot{q}) \\ C_{21}(q,\dot{q}) & C_{22}(q,\dot{q}) \end{bmatrix}; \quad G(q) = \begin{bmatrix} G_1(q) \\ G_2(q) \end{bmatrix} \quad (4)$$

$M(q)$ is symmetric positive definite. The actuated equation 2 shows a direct relationship between the actuated states q_a and the actuators U. By contrast, the unactuated equation 3 does not display the constraint between the unactuated states q_u and the inputs U. Physically, input signals U indirectly drive the actuated states q_a directly and the unactuated states q_u. The system's dynamics, characterized by equations 2 and 3, allow defining a simpler model with an equivalent linear form based on the non-linear feedback method [16], being $M_{22}(q)$ a positive definite matrix. The unactuated states q_u can be determined, from Equation 3, in the following way:

$$\ddot{q}_u = -M_{22}^{-1}(q)\{M_{21}(q)\ddot{q}_a + C_{21}(q,\dot{q})\dot{q}_a + C_{22}(q,\dot{q})\dot{q}_u + G_2(q)\} \quad (5)$$

In underactuated mechanical systems, we can take advantage of the fact that the unactuated state q_u has a geometric relationship with the actuated state q_a. Therefore, control input U indirectly acts on q_u through q_a. Considering the actuated states q_a as the system outputs, the actuated equation 2 can be linearized by defining:

$$\ddot{q}_a = V_a \quad (6)$$

with $V_a \in R^m$ as the equivalent control inputs. Control inputs U are designed to drive the actuated states q_a to the target values q_{ta}. In order to define the profiles of the state trajectories, the following equivalent control inputs are selected:

$$V_a = \ddot{q}_{ta} - K_{da}(\dot{q}_a - \dot{q}_{ta}) - K_{pa}(q_a - q_{ta})$$

(7)

Given that $q_{ta} = const$, Equation 7 can be reduced into

$$V_a = -K_{da}\dot{q}_a - K_{pa}(q_a - q_{ta})$$

(8)

with K_{da} K_{pa} and positive diagonal matrices in $\in R^{m\,x\,m}$. Considering Equation 7 and the definition eq. 6, the differential equation of the control error is obtained by

$$\delta\ddot{q}_a + K_{da}\delta\dot{q}_a + K_{pa}\delta q_a = 0$$

(9)

where $\delta q_a = q_a - q_{ta}$ is the control error vector of the actuated states.

The dynamics of the control error (eq. 9) are exponentially stable for every $K_{da} > 0$ $K_{pa} > 0$. In other words, the control errors of the actuated states δq_a tend to zero as the time t becomes infinite.

4. Mathematical Description of a Harbour Crane System

The crane configuration is characterized by three controlled motions for a harbour crane: a boom displacement, a rotation of the crane about his vertical axis **z** (slewing motion), and a vertical motion along the axis **z** with a variation of the length **l**. Therefore, for describing the motion of the harbour crane, an equivalent kinematics scheme with concentrated masses is represented in Figure 2. Dynamics of the generalized harbour crane are represented as a multi-body system. If we refer to the energy, the following balance can be defined.

4.1. Potential Energy

The Potential energy of the load with mass m is:

$$V_m = -pz + C$$

(10)

Considering the position z along the vertical (with reference to FIGURE2), we have:

$$z = l\cos\varphi_r \cos\varphi_t \quad (11)$$

and, therefore, it is obtained:

$$V_m = -l\left(\cos\varphi_r \cos\varphi_t\right)\left(p\right) \equiv \delta L = -mgl\cos\varphi_r \cos\varphi_t$$

(12)

4.2 Kinetics Energy

The Kinetics energy of the harbour crane is the sum of the corresponding terms for the tower $\mathbf{T_T}$, the boom $\mathbf{T_B}$, and the load $\mathbf{T_L}$.

$$T = T_T + T_B + T_L \tag{13}$$

$$T_T = \frac{1}{2} J_T \dot{\varphi}^2 \tag{14}$$

$$T_B = \frac{1}{2} m_B (r^2 \varphi^2 + \dot{r}^2) \tag{15}$$

$$T_L = \frac{1}{2} m_L v_L^2 \tag{16}$$

In order to simplify the final system of Lagrange equations, we take into account only small sway angles. That means the following assumptions:

$$\sin\varphi_r \approx \varphi_r, \sin\varphi_t \approx \varphi_t, \cos\varphi_r \approx 1, \cos\varphi_t \approx 1 \tag{17}$$

With this assumption, the payload's velocity v_L can be obtained by defining his expression in terms of the Lagrangian coordinates. In this way, it is possible to obtain, for the term $\mathbf{T_L}$, the following expression:

$$T_L = \frac{1}{2} m_L \begin{Bmatrix} \dot{\varphi}^2 (l\varphi_r + r)^2 + (\varphi_r \dot{l} + \dot{\varphi}_r l + \dot{r})^2 + (l\dot{\varphi}\varphi_t)^2 + (\dot{l}\varphi_t + l\dot{\varphi}_t)^2 + \dot{l}^2 + \\ (l\dot{\varphi}_r \varphi_r)^2 + (l\dot{\varphi}_t \varphi_t)^2 + \\ +2\dot{\varphi}(l\varphi_r + r)(\dot{l}\varphi_t + l\dot{\varphi}_t) - 2\dot{\phi}(\varphi_r \dot{l} + \dot{\varphi}_r l + \dot{r})(l\varphi_t) + \\ -2\dot{\varphi}_r \varphi_t l\dot{l} - 2\dot{\varphi}_t \varphi_t l\dot{l} + 2\dot{\varphi}_r \dot{\varphi}_t \varphi_r \varphi_t l^2 \end{Bmatrix} \tag{18}$$

4.3. Lagrange Equations

We now pass to the system given by the equations relating to the dynamics of the harbor crane. Considering the five Lagrangian coordinates q_i described in Section 2, we derive the Lagrange function:

$$L = T - V \tag{19}$$

where T is the Kinetic Energy of the crane system and V the Potential Energy. As a consequence, we apply the generalized Lagrange equations

$$\frac{d}{dt}\left(\frac{\partial L}{\partial \dot{q}_i}\right) - \frac{\partial L}{\partial q_i} = Q_i \tag{20}$$

and so we can obtain the system of equations in the generalized coordinates q_i. In the Lagrange equations (20), the generalized non-conservative Forces Q_i are introduced relative to the dissipative forces. Particularly they can represent the components, on the axes x and y, of air resistance forces acting on both the payload and boom system, the components of the wind force, and the components of the forces due to the damping of the rotation movement. We focus our interest relative to the Lagrangian coordinates r, φ, l φ_r, φ_t, since φ, r and l are directly controlled by the generated profiles that the Plc sent to the axes drives. Assuming the small angles approximation from Lagrange equations (20), we obtain the system of the following five equations, with three actuators used to stabilize five outputs:

$$\begin{aligned} F_r &= (m_B + m_L)\ddot{r} - m_L l\varphi_t \ddot{\varphi} + m_L \varphi_r \ddot{l} + m_L l\ddot{\varphi}_r + k_r \dot{r} \\ &-[m_B r + m_L (r + l\varphi_r)^2]\dot{\varphi}^2 - 2m_L \varphi_t \dot{l}\dot{\varphi} + 2m_L \dot{l}\dot{\varphi}_r \end{aligned} \tag{21}$$

$$\begin{aligned} F_\varphi &= -m_L l\varphi_t \ddot{r} + J_T \ddot{\varphi} + m_L r\varphi_t \ddot{l} + m_L lr\ddot{\varphi}_t + k_\phi \dot{\varphi} \\ &+ 2m_L l\varphi_r \dot{r}\dot{\varphi} + 2m_B r\dot{r}\dot{\varphi} + 2m_L lr\dot{\varphi}\dot{\varphi}_r + 2m_L r\dot{l}\dot{\varphi}_t \end{aligned} \tag{22}$$

$$\begin{aligned} F_l &= m_L \varphi_r \ddot{r} + m_L r\varphi_t \ddot{\varphi} + m_L \ddot{l} + k_l \dot{l} \\ &- m_L r\varphi_r \dot{\varphi}^2 + 2m_L \varphi_t \dot{r}\dot{\varphi} - m_L g \end{aligned} \tag{23}$$

$$\begin{aligned} 0 &= m_L \ddot{r} - m_L l\varphi_t \ddot{\varphi} + m_L l\ddot{\varphi}_r + k_{\varphi_r} \dot{\varphi}_r - m_L (r + l\varphi_r)\varphi^2 \\ &- 2m_L \varphi_t \dot{l}\dot{\varphi} - m_L (\varphi_r / l)\dot{l}^2 + 2m_L \dot{l}\dot{\varphi}_r - 2m_L l\dot{\varphi}\dot{\varphi}_t + m_L \varphi_r g \end{aligned} \tag{24}$$

$$0 = m_L(r + l\varphi_r)\ddot{\varphi} + m_L l\ddot{\varphi}_t + k_{\varphi_t}\dot{\varphi}_t - m_L l\varphi_t\varphi^2 + 2m_L\dot{r}\dot{\varphi}$$
$$+ 2m_L\varphi_r\dot{l}\dot{\varphi} - m_L(\varphi_t/l)\dot{l}^2 + 2m_L\dot{l}\dot{\varphi}_t + 2m_L l\dot{\varphi}\dot{\varphi}_r + m_L\varphi_t g \quad (25)$$

where:

m_L and m_B represent the payload and the Boom mass, respectively;

k_r, k_φ, k_l, k_{φ_r} and k_{φ_t} represent the damping parameters relative to the Lagrangian coordinates, respectively;

J_T represent the inertia momentum of the mast around the z-axis.

F_r F_φ And F_l represent respectively the generalized forces generated by the three actuators;

g is the gravity acceleration.

So, the multiple degrees of freedom boom crane system results are defined by the five differential equations where the terms relative to the Centrifugal and Coriolis forces logically appear.

Harbor crane dynamics can be represented by matrix eq.1, in which the component matrices are determined in the following way:

$$M(q) = \begin{bmatrix} m_{11} & m_{12} & m_{13} & m_{14} & 0 \\ m_{21} & m_{22} & m_{23} & 0 & m_{25} \\ m_{31} & m_{32} & m_{33} & 0 & 0 \\ m_{41} & m_{42} & 0 & m_{44} & 0 \\ 0 & m_{52} & 0 & 0 & m_{55} \end{bmatrix}; \quad C(q,\dot{q}) = \begin{bmatrix} k_r & c_{12} & c_{13} & c_{14} & 0 \\ c_{21} & k_\varphi & 0 & c_{24} & c_{25} \\ c_{31} & c_{32} & k_l & 0 & 0 \\ 0 & c_{42} & c_{43} & c_{44} & c_{45} \\ c_{51} & c_{52} & c_{53} & c_{54} & c_{55} \end{bmatrix}; \quad (26)$$

$$F(q) = \begin{bmatrix} F_r & F_\varphi & F_l & 0 & 0 \end{bmatrix}; \quad G(q) = \begin{bmatrix} 0 & 0 & g_3 & g_4 & g_5 \end{bmatrix}. \quad (27)$$

The elements of the $M(q)$ matrix are the following:

$m_{11} = m_B + m_L$; $m_{12} = -m_L l\varphi_t$; $m_{13} = m_L\varphi_r$; $m_{14} = m_L l$;

$m_{21} = -m_L l\varphi_t$; $m_{22} = J_H$; $m_{23} = m_L r\varphi_t$; $m_{25} = m_L rl$; $m_{31} = m_L\varphi_r$; $m_{32} = m_L r\varphi_t$; $m_{33} = m_L$;

$m_{41} = m_L$; $m_{42} = -m_L l\varphi_t$; $m_{44} = m_L l$; $m_{52} = m_L(r + l\varphi_r)$; $m_{55} = m_L l$.

The elements of the $C(q,\dot{q})$ matrix are the following:

$c_{12} = -[m_B r + m_L(r + l\varphi_r)^2]\dot{\varphi}$; $c_{13} = -2m_l\varphi_t\dot{\varphi}$; $c_{14} = 2m_L\dot{l}$;

$c_{21} = 2m_L(m_l + m_B)(l + r)\dot{\varphi}$; $c_{24} = 2m_L lr\dot{\varphi}$; $c_{25} = 2m_L r\dot{l}$; $c_{31} = 2m_L\varphi_t\dot{\varphi}$; $c_{32} = -m_L r\varphi_r\dot{\varphi}$;

$c_{42} = -m_L(r + l\varphi_r)\dot{\varphi}$; $c_{43} = -m_L(2\varphi_t\dot{\varphi} + \varphi_r\dot{l}/l)$; $c_{44} = 2m_L\dot{l} + k_r$; $c_{45} = -2m_L l\dot{\varphi}$;

$c_{51} = 2m_L\dot{\varphi}$; $c_{52} = m_L(-l\varphi_t\dot{\varphi} + 2\varphi_r\dot{l})$; $c_{53} = -m_L\varphi_t\dot{l}/l)$; $c_{54} = 2m_L l\dot{\varphi}$; $c_{55} = 2m_L\dot{l} + k_t$.

At the end, the elements of the $G(q)$ vector are defined as:

$g_3 = -m_L g$; $g_4 = m_L\varphi_r g$; $g_5 = m_L\varphi_t g$.

4.4. Stability Analysis for a Harbour Crane

Applying the theory proposed in Section 3, we analyze our harbor system's local stability of the internal dynamics eq. 5. In the definition and study of the zero dynamic, we refer to [18] and to [19]. We define the control of the system starting by equations 5 and 9, where: $K_{da} = diag(K_{da1}, K_{da2}, K_{da3})$, $K_{pa} = diag(K_{pa1}, K_{pa2}, K_{pa3})$, $K_{du} = diag(K_{du1}, K_{du2})$, $K_{pu} = diag(K_{pu1}, K_{pu2})$ are the positive matrices of the control gains and $\alpha = \begin{bmatrix} \alpha_1 & 0 \\ 0 & \alpha_2 \\ 0 & 0 \end{bmatrix}$ is a weighting matrix. Therefore, applying matrix equation 5 to the equations of a harbour crane described by the equations from 21 to 25 and developing the above-defined matrices, the zero dynamics of the system are obtained as:

$$0 = \ddot{\varphi}_r + \left(\frac{1}{l}\right)\left\{\left[2\dot{l} + \left(\frac{k_r}{m_L}\right) - \alpha_1 K_{du1}\right]\dot{\varphi}_r + (-2l\dot{\varphi} + l\varphi_t\alpha_2 K_{du2})\dot{\varphi}_t - \varphi_r\alpha_1 K_{pu1} + l\varphi_t^2\alpha_2 K_{pu2} + g\varphi_r\right\} \quad (28)$$

$$0 = \ddot{\varphi}_t + \left(\frac{1}{l}\right)\left\{(2l\dot{\varphi})\dot{\varphi}_r + \left[2\dot{l} + \left(\frac{k_t}{m_L}\right) - (r + l\varphi_r)\alpha_2 K_{du2}\right]\dot{\varphi}_t - \left[(r + l\varphi_r)\varphi_t\alpha_2 K_{pu2}\right] + g\varphi_t\right\} \quad (29)$$

The stability of the zero dynamics is analyzed using the linearization theorem of Lyapunov. As a consequence of eq. (27) and (28), in the paper [13], we establish the constraint conditions for the controller parameters, which result necessary to define the stability of the system.

4.5. Hydraulic Cylinder Cinematics

Typically, the works relative to harbour cranes do not consider the actuator dynamics and kinematics. Nevertheless, being a harbour crane driven by hydraulic actuators, the kinematics of the actuators is not negligible. Specifically, the kinematics of the same actuators must be considered for the boom actuator.

Following, the actuator's kinematics for the boom's radial direction are described. Here, we will assume that the hydraulic cylinder has first-order behaviour. Therefore the differential equation of motion of the hydraulic cylinder is:

$$\ddot{\zeta}_{cyl} + \frac{1}{T_F}\dot{\xi}_{cyl} = \frac{K_{VF}}{T_F \cdot \sigma_{cyl}} v_F \quad (30)$$

Where $\ddot{\zeta}_{cyl}$ and $\dot{\xi}_{cyl}$ are the cylinder acceleration and velocity, T_F the time constant relative to the flow rate, σ_{cyl} the cross-sectional area of the cylinder, v_F the input voltage of the servo-valve, and K_{VF} the constant of proportionality between the flow rate and the input voltage v_F.

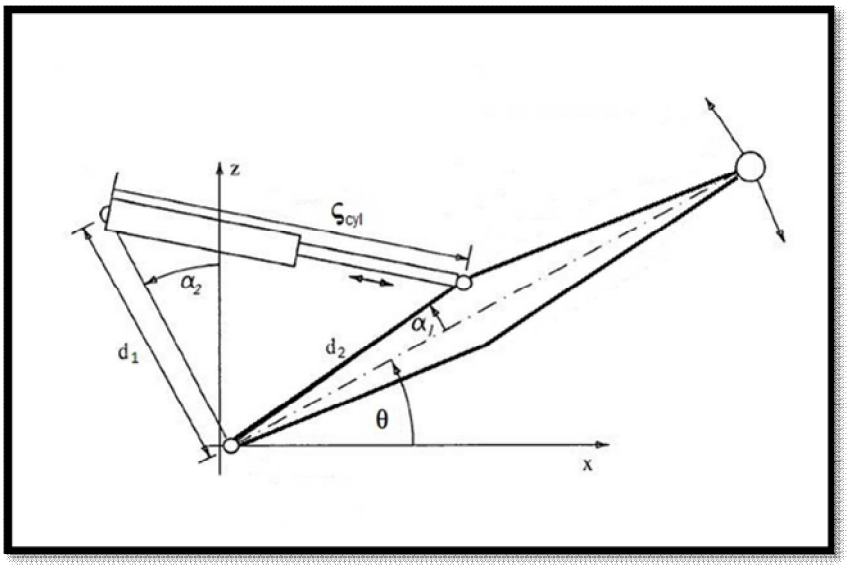

Figure 3: Geometric Description of the Hydraulic Cylinder Cinematics

Observing Figure2 and Figure3, it is possible to obtain the relation between the radial position of the end of the boom r and the cylinder coordinate ζ_{cyl}:

$$r(\zeta_{cyl}) = L \cdot \cos\vartheta \quad (31)$$

Being: $\vartheta = \frac{\pi}{2} + \alpha_2 - \alpha_1 - \arccos\left(\frac{d_1 + d_2 - \zeta_{cyl}^2}{2d_1 d_2}\right)$ (32)

Differentiating, we obtain:

$$\dot{r} = -L \cdot \sin\vartheta \cdot K_1(\vartheta) \cdot \dot{\xi}_{cyl} \quad (33)$$

$$\ddot{r} = -L \cdot \sin\vartheta \cdot K_1(\vartheta) \cdot \ddot{\zeta}_{cyl} - K_2(\vartheta) \cdot \dot{\xi}_{cyl}^2 \quad (34)$$

Where K_1 and K_2 define the relation between the geometric constants d_1, d_2, α_1, α_2 and the luffing angle ϑ. L is the length of the boom. Therefore, we obtain the input voltage of the servo-valve v_F as a function of $\dot{r}$ and $\ddot{r}$.

Defining:

$$A \equiv \frac{T_F \cdot \sigma_{cyl}}{K_{VF}} \quad (35)$$

$$B \equiv l \cdot \sin\vartheta \cdot K_1(\vartheta) \quad (36)$$

We obtain:

$$v_F = -A \cdot \left\{ \frac{\ddot{r}}{B} + K_2 \frac{\dot{r}^2}{B^2} + \left(\frac{1}{T_F} \right) \frac{\dot{r}}{B} \right\} \quad (37)$$

Eq.37 allows obtaining the input voltage of the servo-valve v_F as a function of $\dot{r}$ and $\ddot{r}$.

5. Equation Solution

Since our goal is to obtain a strategy to reduce the oscillatory motion of the rotary crane payload, we will concentrate on equations 24 and 25 involving the two variables φ_r and φ_t corresponding to the two oscillatory degrees of freedom. In fact, we want to point out that a rotation movement generates two components of sway in contrast to linear movements. This sway angle exhibits non-zero components φ_r and φ_t corresponding to the two oscillatory degrees of freedom in the two perpendicular directions, r, and t. The second component φ_t, along the tangential direction to the slewing movement, is generated by the variation of the velocity of the suspension point and can be eliminated by acting only on the control of the rotation movement. Instead of this, the other component φ_r along the radial direction is generated by the centrifugal force. This force causes a load movement that is directed along a perpendicular plane XZ. Therefore, the component φ_r cannot be eliminated by acting on the control of the rotation movement. Disregarding the terms of superior order in equations 24 and 25 and considering all the trigonometric terms, we obtain:

$$\ddot{\varphi}_r = -\frac{1}{l} \left\{ \begin{array}{l} \ddot{r} - l\varphi_t \ddot{\varphi} - \left(r + l\varphi_r \right) \varphi^2 - 2\left(l\dot{\varphi}_t + \dot{l}\varphi_t \right) \dot{\varphi} \\ + \left[2\dot{l} + \left(\frac{k_r}{m_L} \right) \right] \dot{\varphi}_r - \left(\frac{\varphi_r}{l} \right) \dot{l}^2 + g\varphi_r \end{array} \right\} \quad (38)$$

$$\ddot{\varphi}_t = -\frac{1}{l} \left\{ \begin{array}{l} (r + l\varphi_r)\ddot{\varphi} - l\varphi_t \varphi^2 + 2\left(\dot{r} + l\dot{\varphi}_r + \dot{l}\varphi_r \right) \dot{\varphi} \\ + \left[2\dot{l} + \left(\frac{k_t}{m_L} \right) \right] \dot{\varphi}_t - \left(\frac{\varphi_t}{l} \right) \dot{l}^2 + g\varphi_t \end{array} \right\} \quad (39)$$

Where k_t and k_r are the friction coefficients with a fixed value, depending on the considered axis. $\dot{l}$ is the derivative of the length l (that is the velocity of the vertical movement along the axis Z). $\ddot{r}$ is the acceleration of the boom movement along the axis X. $\ddot{\varphi}$ is the angular acceleration of the slewing movement along the tangential direction to the slewing. $\dot{r}$ is the acceleration of the boom movement along the radial direction. $\dot{\varphi}$ is the angular velocity of the slewing movement along the tangential direction. g is the gravity acceleration and m_L is the mass of the payload.

The control device calculates the angles φ_r φ_t of the load's oscillation and angular velocities $\dot{\varphi}_r$ and $\dot{\varphi}_t$ of the same sway angles. Practically, the control method calculates the described data through an iterative process using the velocity and acceleration of the sway angles. The calculation uses Equations 38 and 39 to define the successive steps. The subsequent steps are obtained with an iterative method that can be represented, at any time t, in the following way. Starting from equation 39 φ_t, $\dot{\varphi}_t$ and $\ddot{\varphi}_t$ represent the internal variable. They are obtained with an iterative method that can be represented, at any time t, in the following way:

$$\ddot{\varphi}_t = \left(\dot{\varphi}_t - \dot{\varphi}_{t-1} \right) \cdot \Delta t \quad (40)$$

$$\dot{l}_t = \left(l_t - l_{t-1} \right) \cdot \Delta t \quad (41)$$

$$\ddot{\varphi}_{t,t} = -\frac{1}{l_t} \left\{ \begin{array}{l} (r_t + l_t\varphi_{r,t})\ddot{\varphi}_t - l_t\varphi_{t,t}\varphi_t^2 + 2\left(\dot{r}_t + l_t\dot{\varphi}_{r,t} + \dot{l}_t\varphi_{r,t} \right) \dot{\varphi}_t \\ + \left[2\dot{l}_t + \left(\frac{k_t}{m_L} \right) \right] \dot{\varphi}_{t,t} - \left(\frac{\varphi_{t,t}}{l_t} \right) \dot{l}_t^2 + g\varphi_{t,t} \end{array} \right\} \quad (42)$$

$$\dot{\varphi}_{t,t} = \dot{\varphi}_{t,t-1} + \ddot{\varphi}_{t,t} \cdot \Delta t \quad (43)$$

$$\varphi_{t,t} = \varphi_{t,t-1} + \dot{\varphi}_{t,t-1} \cdot \Delta t \quad (44)$$

In these equations $\dot{\varphi}_{t,t}$ and $\dot{\varphi}_{t,t-1}$ represent the velocity of the sway angle along the tangential direction, respectively, at the time t and at the previous time t-1. $\ddot{\varphi}_{t,t}$ $\ddot{\varphi}_{t,t-1}$ represent the acceleration of the sway angle along the tangential direction respectively at the time t and at the previous time t-1. In equation 42, $\ddot{\varphi}_t$ represent the angular acceleration of the movement of the slewing axis at the time t. In equation 40, $\dot{\varphi}_t$ and $\dot{\varphi}_{t-1}$ represent the angular velocity of the movement of the slewing axis respectively at the time t and at the previous time t-1. $\dot{l}_t$ Represent the velocity of the

movement of the hoisting relative to the Z vertical direction at the time t. l_t and l_{t-1} represent the length of the cable respectively at the time t and at the previous time t-1. Δt Represent the time difference between the instant t and the instant t-1.

The iterative process starts with the hypothesis that at the initial instant, the values of the sway angle φ_t, the velocity of the sway angle, $\dot{\varphi}_t$ and the acceleration of the sway angle $\ddot{\varphi}_t$ are equal to zero; that is, the pendulum is initially in quiet conditions.

Therefore, for t=0, we have:

$$\varphi_{t,0} = \dot{\varphi}_{t,0} = \ddot{\varphi}_{t,0} = 0 \quad (45)$$

The considerations defined for Equation 39 can be repeated similarly for equation 38 relative to the radial sway angle φ_r.

The control device can control, at the same time, the movements along the axis X, Y, and Z, being the axis Z, the vertical axis relative to the hoisting movement. To synchronize this model with the real crane, an observer must be designed to verify that the system is observable. We can determine the eigenvectors and corresponding eigenvalues using the Observer method applied to Equations 38 and 39. As a consequence, the observer gain matrix is obtained. Specifically, we obtain the correction $\Delta\dot{\varphi}$ of the angular velocity of the movement along the tangential direction according to the following equation:

$$\Delta\dot{\varphi} = K_{0,\phi} \cdot \varphi_t + K_{1,\phi} \cdot \dot{\varphi}_t \quad (46)$$

wherein $K_{0,\varphi}$ and $K_{1,\varphi}$ are the observer gains applied respectively to the sway angle φ_t and to the velocity $\dot{\varphi}_t$ of the sway angle $\Delta\dot{\varphi}$ is the correction signal that is added to the velocity set-point $\dot{\varphi}_{set}$. Therefore, the reference of velocity applied as input to the inverter driving the motor relative to the slewing movement is the angular velocity set $\dot{\varphi}_{ref}$ that is obtained in the following way:

$$\dot{\varphi}_{ref} = \dot{\varphi}_{set} + \Delta\dot{\varphi} \quad (47)$$

The $K_{0,\varphi}$ and $K_{1,\varphi}$ observer gains are function of the cable length to optimize the velocity corrections according to the pendulum's length.

In the same way, we obtain the correction $\Delta\dot{r}$ of the velocity of the movement along the radial direction.

6. Implementation and Results

As a consequence of his simplicity, the control device can be integrated into a Plc. The correction method uses the calculated values of the sway angles and the sway angles velocities to compute the correction at the boom and slewing velocity to add to the set-point velocities (arriving from the operator or defined automatically), obtaining in this way the speed profiles. A drive controller generates the speed profiles of the movements relative to the boom (Boom movement) and the slewing (Slewing movement) and supplies the speed profile information to the drive able to control the corresponding motor. The cyclic task, where the Function Block of the used Plc was realised, had a time of updating equal to 30 ms.

The Function Blocks (FBs) used were two. The first FB computes the speed profiles necessary to obtain the anti-sway functionality and the corresponding actual sway angles. The second FB is used to compute the actual length l of the cable and the corresponding vertical speed using the data coming from external units (i.e., encoders) connected to the motor of the corresponding movement.

The Speed reference is the target value to which the speed must arrive, defined by the crane operator or from the automatic control. Usually, it is defined in Hz as a consequence of how the electric motors are built. At speed in Hz on the fast shaft (that is on the motor), a velocity corresponds on the slow shaft (that is on the boom moved by the hydraulic system or on the shaft controlling the slewing motion of the jib), depending on the reduction gearing from the motor to the cinematic actuators. Typically, the max speed of the boom can be from 0.2 m/s to also more than 2 m/s. The max speed of a slewing motion (measured in rad/s) can arrive at 0.5 rad/s. The Ramp Set is the time value necessary for a linear motor ramp to reach the speed reference.

Based on the speed reference, the estimator module computes the real speed profile to have the anti-sway effect. The speed profile is longer than the linear Ramp Set. The cable length has a very important influence on the speed profile because the greater the height (and so the cable length), the greater the time of the speed profile. In a general way, it is very important to reduce the time of the speed profile to obtain a fast answer to the commands of the boom crane movement.

In Figure 4, we can see the profiles of the angular velocity profile for the slewing movement and the corresponding profile of the tangential sway angle.

Some subsequent commands (4) are shown to go to different velocities (but not zero velocity) for the slewing movement in Figure 5. We can see that the corresponding sway angles go to zero at the end of the movement. Therefore, we see that, with this method, it is possible to obtain the total damping of the sway changing many times the velocity set, also if the previous damping control of the oscillations is again in progress (see Figure 5). That is fundamental because the

usual control of the boom crane is typically manual by a human operator: typically, he will often change the target velocity with his command.

Many of the previous works, under open-loop control, typically use the 'model predictive control,' which is an optimized method for automatic control, where there is a pre-defined position target. However, the method defined in this work is preferable when the control is manual.

An important characteristic is highlighted in Figure 6. Varying some basic parameters for the profiles, the same profiles for the velocity can be fast, mainly corresponding to a very fast stop with an anti-sway. This is a relevant result to control the crane with high performance related to the answer at the command.

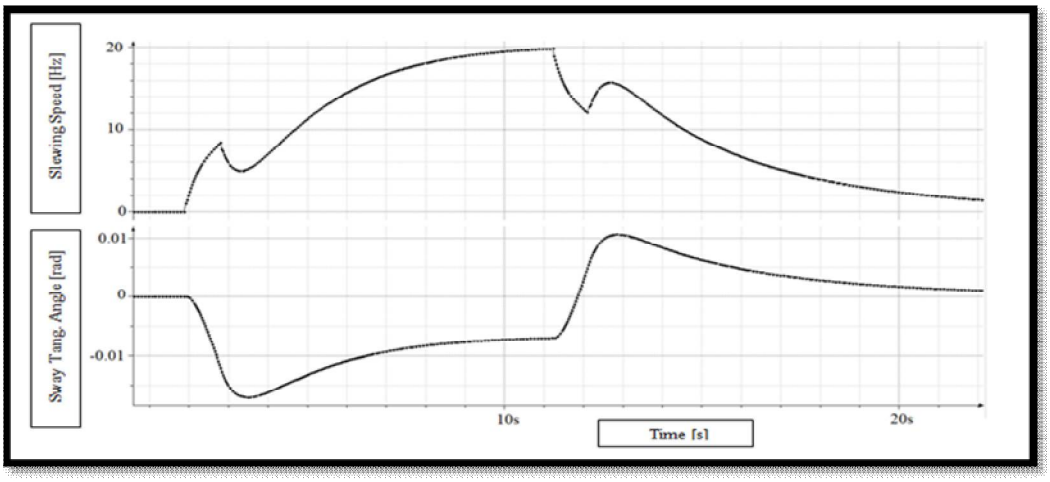

Figure 4: It Shows a Graph Relative to the Angular Velocity Profile $\dot{\varphi}_{ref}$ of the Slewing Movement and the Tangential Sway Angle Corresponding Profile φ_t. That Is in Correspondence to a Command Relative to the Only Slewing Movement. The Specific Values Are: Speed Reference = 25 Hz, Ramp Set=1.5s, Cable Length=10.5 M, Cycle Time of the Plc=30ms.

7. Conclusion

In this paper, we investigate the sway control of a harbor crane. An open-loop solution for the effective non-linear equations of motion is obtained by defining an iterative method for the solution of the movement equation. The present work considers the continuous variation of the hoisting height for the suspension point of the payload and the corresponding velocity and acceleration variation.

After having defined the stability of the proposed solution, and the kinematics of the hydraulic actuators on the boom, a detailed mathematical model is developed, considering the non-linear components of the forces, such as centrifugal and Coriolis forces on the system. The multiple-input and multiple-output (MIMO) mechanical system is modeled by a set of non-linear differential equations in which the mathematical model is divided into two subsystems: the first for actuated outputs and the second for underactuated outputs.

An implementation of the method and the most relevant results are described.

Possible future developments of this work may concern the study of the effect relative to external disturbances such as wind or sea waves. These effects involve the use of a closed-loop solution.

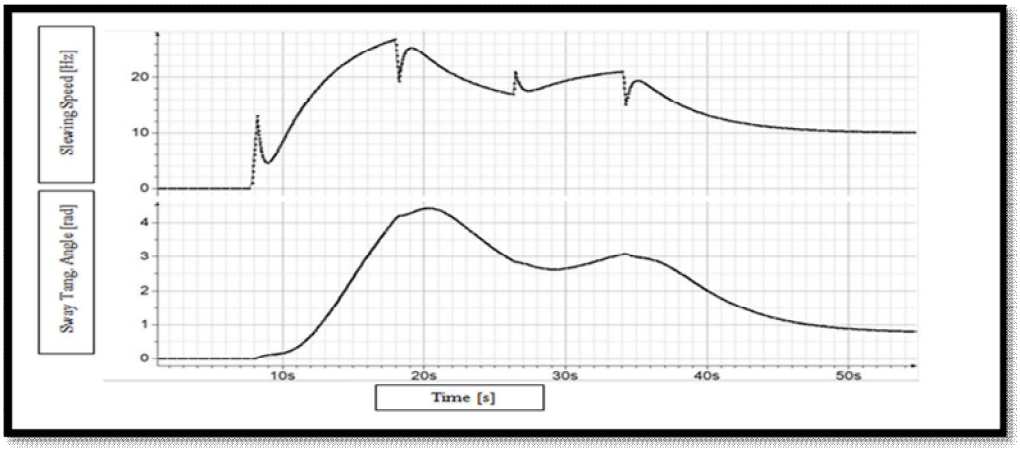

Figure 5: It Shows a Graph Relative to the Angular Velocity Profile $\dot{\varphi}_{ref}$ of the Slewing Movement and the Tangential Sway Angle Corresponding Profile φ_t. That Is in Correspondence to Some Subsequent Commands of the Slewing Movement by the Operator. The Specific Values Are: Initial Slewing Speed Reference = 30 Hz, Final Slewing Speed Reference = 10 Hz Ramp Set=1.5s, Cable Length=10.5 M, Cycle Time of the Plc=30ms.

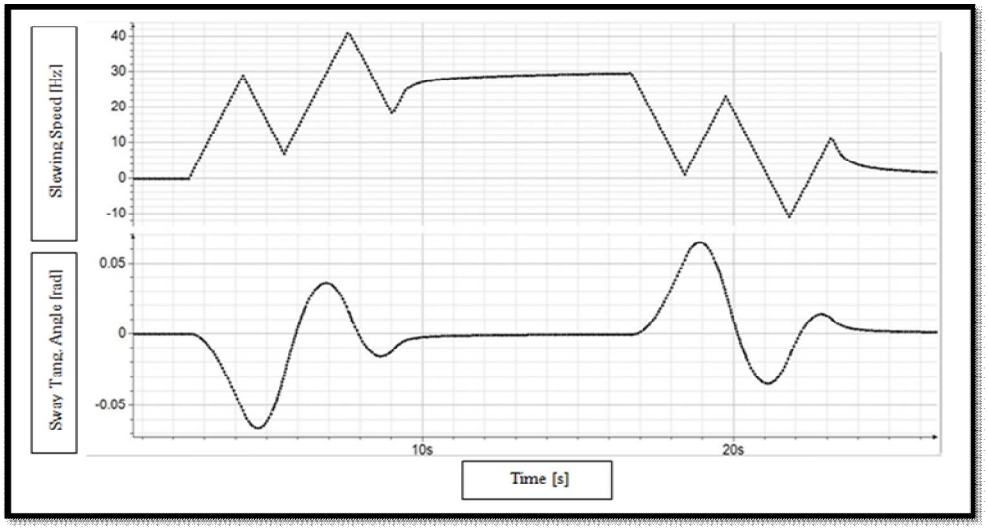

Figure 6: It shows a Graph Relative to the Angular Velocity Profile $\dot{\varphi}_{ref}$ of the Slewing Movement and the Tangential Sway Angle φ_y Corresponding Profile. That Is in Correspondence to a Command Relative to the Only Slewing Movement. The Specific Values Are: Speed Reference = 30 Hz, Ramp Set=3.0s, Cable Length=10.5 M, Cycle Time of the Plc=30ms.

8. References

i. Ramli, L. & Mohamed, Z. & Abdullahi, A. & Jaafar, H.I. & Lazim, I.M. (2017). Control strategies for crane systems: A comprehensive review. *Mechanical Systems and Signal Processing*, *95*, 1–23. DOI: 10.1016/j.ymssp.2017.03.015.

ii. Caporali, R.P.L. (2018). Iterative Method for controlling with a command profile the Sway of a Payload for Gantry and Overhead Travelling Cranes. *International Journal of Innovative Computing, Information, and Control*, *14* (3), 1095-1112. DOI: 10.24507/ijicic.15.04.1223.

iii. Caporali, R.P.L. (2019). Overhead Crane: an adaptive Particle Filter for anti-Sway closed-loop and collision detection using Computer Vision. *International Journal of Innovative Computing, Information, and Control*, *15* (4), 1223-1241. DOI: 10.24507/ijicic.15.04.1223.

iv. Caporali, R.P.L. (2018). Iterative Method for controlling the sway of a payload on tower (slewing) cranes using a command profile approach. *International Journal of Innovative Computing, Information and Control*, *14* (4), 1169-1187. DOI: 10.24507/ijicic.14.04.1169.

v. Caporali, R.P.L. (2021). Anti-sway method for reducing vibrations on a tower crane structure. *International Journal of Nonlinear Sciences and Numerical Simulation*. https://doi.org/10.1515/ijnsns-2021-0046.

vi. Kim, D. & Park, Y. & Kwon, S.& Kim, E. (2011). Dual stage trolley control system for anti-swing control of mobile harbor crane. *11th Int. Conf. Control. Autom. Syst.*, South Korea, 420-423.

vii. Sun, Y.G. & Quiang, H.Y. & Xu, J. & Dong, D.S. (2017). The non-linear dynamics and anti-sway tracking control for offshore container crane on a mobile harbor. *Journal of Marine Science and Technology*, 656-665. DOI: 10.6119/JMST-017-1226-05.

viii. Arnold, E. & Sawodny, O. & Neupert, J. & Schneider, K. (2005). Anti-sway system for boom cranes based on a model predictive control approach. *IEEE Int. Conf. Mechatronics Autom.*, Ontario, Canada. 1533-1538.

ix. Neupert, J. & Arnold, E. & Schneider, K. & Sawodny, O. (2010). Tracking and anti-sway control for boom cranes. *Control Eng. Pract.*, *18*, 31-44.

x. Toyohara, T. & Shimotsu, T. & Iwamoto, N. & Yoshioka, N. (2003). Anti-Sway Control for Jib Cranes. *The Proceedings of the Transportation and Logistics Conference*, *12*, 149-150. DOI:10.1299/jsmetld.2003.12.149.

xi. Kim, D. & Park, Y. (2015). 3-Dimensional position control scheme for mobile harbor crane. *15th Int. Conf. Control. Autom. Syst. Proc.*, Busan, South Korea, 202-216.

xii. Huang, J. & Maleki, E. & Singhose, W. (2013). Dynamics and swing control of mobile boom cranes subject to wind disturbances. *IET Control Theory and Applications*, *7* (9), 1187–1195. DOI: 10.1049/iet-cta.2012.0957.

xiii. Caporali, R.P.L. (2022). Analysis of the System Stability for an anti-Sway method relative to Harbor Cranes. *International Journal of Recent Engineering Research and Development*, *7* (6), 35-45.

xiv. Tuan, L.A. & Lee, S.G. (2016). Nonlinear Feedback Control of Underactuated Mechanical Systems. *IntechOpen*, *10*. DOI: http://dx.doi.org/10.5772/64739.

xv. Tuan, L.A. & Lee, S.G. & Dang, V.H. & Moon, S. & Kim, B.S. (2013). Partial Feedback Linearization Control of a Three Dimensional Overhead Crane. *International Journal of Control, Automation, and Systems*, *11* (4), 718-727.

xvi. Spong, M.W. (1994). Partial feedback linearization of under-actuated mechanical systems. *Proceedings of the International Conference on Intelligent Robots and Systems*, Munich.

xvii. Lefeber, E. & Pettersen, K.Y. & Nijmeijer, H. (2003). Tracking Control of an Under-actuated hip. *IEEE Transactions on Control Systems Technology*, *11* (1), 52-61.

xviii. Slotinne, J.E. & Li, W. (1991). *Applied Nonlinear Control*, New Jersey: Prentice Hall.

xix. Ogata, K. (2010). *Modern Control Engineering*. New Jersey: Prentice Hall.